EuroSun 2022

CHARACTERIZATION OF ENHANCED BIOBASED PHASE CHANGE MATERIAL WITH GRAPHENE NANOPLATELETS – EARLY RESULTS

Elisangela J. D'Oliveira[1], Sol Carolina Costa Pereira[1], Dominic Groulx[2], Ulugbek Azimov[1]

[1]Department of Mechanical Engineering at Northumbria University at Newcastle

[2]Department of Mechanical Engineering at Dalhousie University

Abstract

Energy consumption is expected to continue rising, and in conjunction with greater environmental concern, it has boosted the development of renewable and sustainable energy sources, including storage media materials for thermal energy storage (TES) systems. Biobased Phase Change Materials (PCMs) are materials derived from renewable and environmentally friendly resources, such as palm oil, and are a great solution as they have similar properties to paraffin-based PCMs. Therefore, in view of designing a nano-enhanced PCMs (NePCMs) based on a commercial plant-based PCM, CrodaTherm60, was selected due to its high latent heat capacity as well as its medium melting point, 60 °C, making it suitable for solar domestic hot water systems (SDWHs). Whilst the selected PCM has desirable properties, it still possesses the most common limitations, such as its low thermal conductivity; thus, NePCMs were prepared and characterized using carbon-based nanoparticles, and graphene nanoplatelets (GNPs).

Keywords: Heat storage, biobased PCM, Thermal properties, Graphene nanoplatelets (GNP), Thermal conductivity.

1. Introduction

Thermal energy storage (TES) systems facilitate the energy balance between energy demand and supply, by storing the renewable energy when its available and release it when demand becomes higher. Energy demands for the residential sector vary seasonally; thus, incorporating a TES is essential for increasing renewable energy utilization. Currently, paraffin-based are the most studied type of organic PCMs for Latent Heat Thermal Energy Storage (LHTES) applications due to their favourable characteristics (Shi et al., 2013), which includes their high latent heat storage capacity and small temperature variation during the phase change process. However, these materials are not obtained from renewable sources, and their carbon footprint impact is often overlooked. Thereby, biobased PCMs are a promising alternative as they could have similar properties as paraffin waxes; thusly, over the recent years the research on this type of PCMs have grown exponentially (Wuliu et al., 2021, Liu et al., 2020, Hu et al., 2021).

Okogeri and Stathopoulos (2021) reviewed the research status of biobased PCMs with a focus on their promising perspectives as well as limitations and drawbacks; they also discussed the possibility of using waste materials such as waste cooking oil as potential alternatives to edible oil-based PCMs. Although biobased PCMs have many desirable properties, they still possess similar drawbacks as paraffin-based PCMs, such as

low thermal conductivities. Thus, methods to improve the thermal conductivity of PCMs are widely investigated, and one of the methods often implemented is the incorporation of high conductive nanoparticles. Different nanoparticles have been studied to improve the thermal conductivity of the PCMs by different researchers (Jeong et al., 2013, Yu et al., 2014, D'oliveira et al., 2022), including nanoparticles based on carbon (Jeong et al., 2013, Yu et al., 2014), metal (Zhang et al., 2021, Cui et al., 2016), and metal oxides (Wang et al., 2012, Manoj Kumar et al., 2020).

Among carbon-based particles, graphene provides excellent properties for enhancing the heat transfer processes in the PCMs, such as high thermal conductivity, 5300 W/m.K (Sang et al., 2019), high aspect ratio and relatively low densities. Prado and Lugo (2020) developed and compared NePCMs based on PureTemp 8 as the PCM, provided by Entropy Solutions, with dispersions of GNPs (11-15 nm thickness) and MgO (35 nm diameter) nanoparticles purchased from IoLiTec; acetic acid, provided by Sigma-Aldrich, was used as a surfactant to improve the stability of the dispersions. Their results showed that more significant thermal conductivity improvements were obtained using GNPs as the conductive filler instead of MgO. Amin (2017) prepared and investigated NePCMs based on Beeswax as PCM and GNPs as nanoparticles, with a particle size of 2 nm. Including 0.3 wt% of GNPs into the PCM increased the thermal conductivity of the composite to 2.8 W/m.K, 11 times higher than the pure beeswax (0.25 W/m.K). Besides that, the inclusion of GNPs not only had a positive effect on the thermal conductivity of the Beeswax but also enhanced the latent heat of the material. Shi et al. (2013) prepared and investigated the thermal conductivity enhancement of paraffin, with a melting temperature of 61.6°C, with loadings of exfoliated graphite nanoplatelets (xGnP) and graphene. From the results obtained by the authors, the thermal conductivity enhancement with graphene was much smaller than expected, and they suggested that the reason was the interfacial thermal resistance because of the inefficient coupling of acoustic waves through the weak van der Waals interaction.

Although many studies were conducted with similar carbon-based nanoparticles, there are significant discrepancies, making the selection of the appropriate nanomaterial for a specific PCM unclear. To the best of authors' knowledge, regarding the preparation and characterization of NePCMs based on CrodaTherm60 as the PCM, no studies were found in the literature; however, researchers have investigated the thermal performance of latent heat thermal energy storage (LHTES) filled with CrodaTherm60 in systems such as multi-tube finned copper heat exchanger (Fadl and Eames, 2021). In the current study, NePCMs based on the commercially available PCM, CrodaTherm60, were incorporated with 2, 4 and 6 wt.% of GNPs through the magnetic stirring and ultrasonication synthesis process. Moreover, to study the effects of the different mass fractions of GNPs on the thermal performance of the CrodaTherm60, the main thermophysical properties, phase change temperatures, latent heat, densities, and thermal conductivity were studied experimentally.

2. Methodology

2.1 Materials

CrodaTherm60 a bio-organic PCM (derived from plant-based feedstock), with a melting temperature of 60 °C supplied by CRODA Energy Technologies was used as the PCM in this study. The thermal properties of the commercially available biobased PCM are shown in Tab. 1, To increase the thermal conductivity of the PCM, graphene nanoplatelets, with a thickness of 2 nm and specific surface area of 750 m^2/g, supplied from IoLiTec were used as the high conductive particles.

Tab. 1: Thermal properties of the commercially available CrodaTherm60

Density [kg/m^3]	Melting Temp. [°C]	Latent heat [kJ/kg]	Thermal conductivity [W/m.K]	Specific heat [kJ/kg. K]
922	60	217	0.29	2.3

2.2 Preparation of NEPCMs

The NePCMs were prepared following the magnetic stirring and ultrasonication process, which offers better incorporation of GNPs nanoparticles into the base of the CrodaTherm60 (Yu et al., 2014, Putra et al., 2017). First, 50 grams of CrodaTherm60 were melted in a water bath at a constant temperature of 80 °C. Afterwards, GNPs nanoparticles were incorporated into the melted PCM and mixed for 30 min with a magnetic stirring at 800 r/min and 80 °C. Having completed the first step of the synthesis process, the melted NePCMs were ultrasonicated in an ultrasonic bath for 30 min at the same temperature to break down the GNPs aggregation and to improve the dispersion of the nanoparticles into the base PCM. The synthesis process implemented in this study is illustrated in Fig. 1.
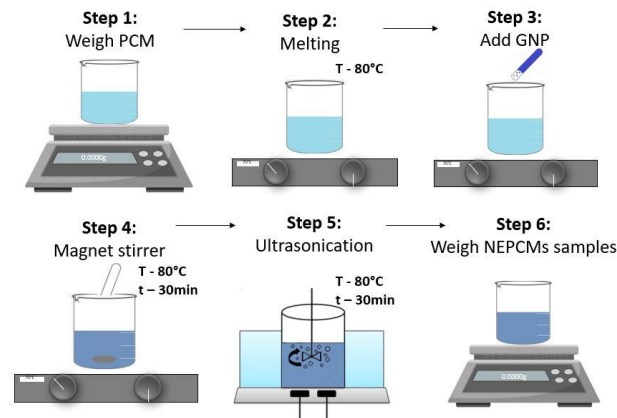

Fig. 1: Procedure of the NEPCMs sample preparation

2.3 Characterization techniques

The morphology and microstructure of the thermal enhanced CrodaTherm60 were observed using scanning electron microscopy (SEM, TESCAN MIRA3) at room temperature. The NePCMs samples were coated with a platinum coating, 5 nm in thickness, to increase the electrical conductivity of the samples. The SEM images were taken at an accelerating voltage of 5kV and the same view field.

Thermal properties of the PCM and NePCM, such as melting and crystallization temperature, latent heat and specific heat capacity, were measured using the Differential Scanning Calorimetry (DSC, 131 SETARAM). The DSC measurements were performed at two heating and cooling rates, 2 K/min and 10 K/min, in a temperature range of 15 to 90 °C for heating and 90 to 15°C for cooling, under a constant stream of argon gas atmosphere and nitrogen to better control heating and cooling rates. Three samples of 7-9 mg of each NePCMs were prepared using a balance with a precision of 0.1 mg.

The thermal conductivity of PCMs and NePCMs were measured by a thermal conductivity instrument (Linseis THB 100), with a measurement accuracy of 5 %. The samples prepared were 50mm x 25 mm with an average thickness of 5mm. The hot point sensor was placed between two samples, and a weight of about 2 kg was used to improve the contact with the sensor. The sensor was calibrated using polymethyl methacrylate (PMMA) with thermal conductivity of 0.194 W/m.K for a single-point calibration. The thermal conductivity was measured at room temperature, solid phase. Several measurements were taken for each sample, and the position of the sensor was changed each time, and the reported values were the mean. The uncertainty for the thermal conductivity reported was estimated to be less than 5 %.

The density of the solid samples was measured using the Arquimedes principles. The method is described in the BS EN ISO 1183-1 standard. The liquid used was ethanol at a temperature of 20 °C. The uncertainty for the density reported was estimated to be less than 1 %.

3. Results and Discussion

3.1 Morphology and microstructure of the NePCMs

The NePCMs samples prepared with 2, 4 and 6 wt.% mass fractions of Graphene nanoplatelets are shown in Fig. 2. The SEM images of the prepared NePCMs presented in Fig. 3, show that the GNPs are well dispersed. However, there is a significant agglomeration shown by the SEM images; with 2 wt.% of GNPs in the based PCM the clustering size was in the microscale and not nanoscale. It is observed that the agglomeration of the nanoparticles increases with the mass concentration of nanoparticles. As seen in Fig. 3 (b) and (c) the GNPs are separated into layers which could limit the formation of an effective heat conduction network.
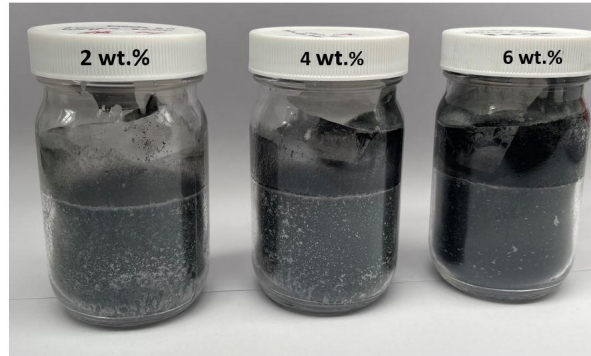

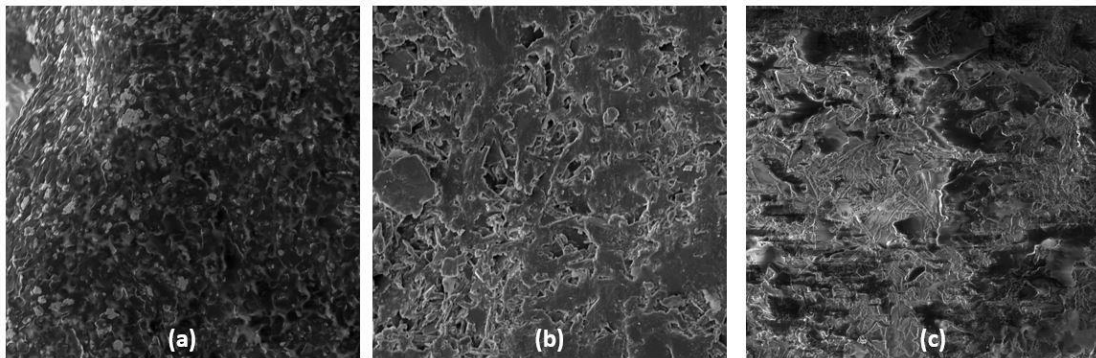**Fig. 2: NePCMs with mass fractions of 2, 4 and 6 wt.% GNPs**

Fig. 3: SEM images of NePCMs with (a) 2 wt.%, (b) 4 wt.% and (c) 6 wt.% with a view field of 100 μm at a 5.0 kV

3.2 Thermal properties of the CrodaTherm60 and CrodaTherm60 NePCMs

The following thermal properties of the pure and enhanced phase change materials were investigated, including the onset temperature and latent heat capacity of melting and solidification processes obtained by the DSC equipment. The first cycle, at 10 K/min, was discarded to eliminate the thermal history of the sample before the measurements were taken; the consecutive cycles were effectively used to avoid discrepancies and outliers. The measurements for the latent heat capacity (ΔH) were taken at 10 K/min, as at this scanning rate the error is minimized, while at 2 K/min, the phase change transition (onset) value tends to be more accurate; thus, testing the samples at both heating rates allowed more accurate identification of the latter thermal properties stated (Müller et al., 2020). The detailed data obtained by the DSC measurements and the estimated latent heat capacity are shown in Tab. 2. It is expected that the addition of GNPs into the CrodaTherm60, will reduce the latent heat capacity of the NePCMs as the content of the base PCM is reduced. Theoretically, the reduction in the latent heat capacity of the NePCMs is directly proportional to the increase in the mass fraction of the additive content and can be calculated with the following equation (Feng et al., 2022, Yuan et al., 2016a):

$$\Delta H_{NePCM} = \varphi \Delta H_{PCM}$$

Where ΔH_{NePCM} is the latent heat of NePCMs, φ is the percentage of PCM and ΔH_{PCM} is the latent heat capacity of the PCM.

Tab. 2: Heat storage properties of CrodaTherm60 and thermal enhanced CrodaTherm60

Material	Wt.%	T_m [°C]	ΔH_m [kJ/kg]	Reduction in ΔH_m [%[	Theoretical ΔH_m [kJ/kg]	T_s [°C]	ΔH_s [kJ/kg]
CrodaTherm 60/ 2nm GNP	0	57.2±0.2	201.7±15.8	-	-	58.1±0.1	209.0±19.9
	2	57.5±0.3	183.6±6.7	-8.98%	197.7	58.3±0.1	186.9±9.1
	4	57.7±0.8	174.8±7.2	-13.34%	193.7	58.4±0.1	180.9±3.3
	6	57.3±0.1	178.5±10.4	-11.51%	189.6	58.4±0.1	183.6±8.8

The melting and solidification curves from the DSC measurements of CrodaTherm60 and the NePCMs with the different mass fractions of GNPs are shown in Fig. 4 (a). The DSC curves of the three NePCMs are similarly shaped to the pure CrodaTherm60, with an observably endothermic peak in the melting process and an exothermic peak in the solidification process. The latent heat capacity for melting and solidification is obtained by integrating the total area under the peaks for the solid-liquid transition curves of the NePCMs. The measured melting temperature of CrodaTherm60 is 57.2 °C, thus, the material is suitable to be used in domestic space and water heating systems. The melting and solidification latent heat are measured as 201.7 and 209.0 kJ/kg, respectively. The supplier, Croda Technologies, provides information about the melting temperature and latent heat (Tab. 1Tab.1) which can be compared to the measured values. In average, the deviaton from the supplier stated values for melting temperature is 4.7 %, however, for latent heat is 7.3 %.
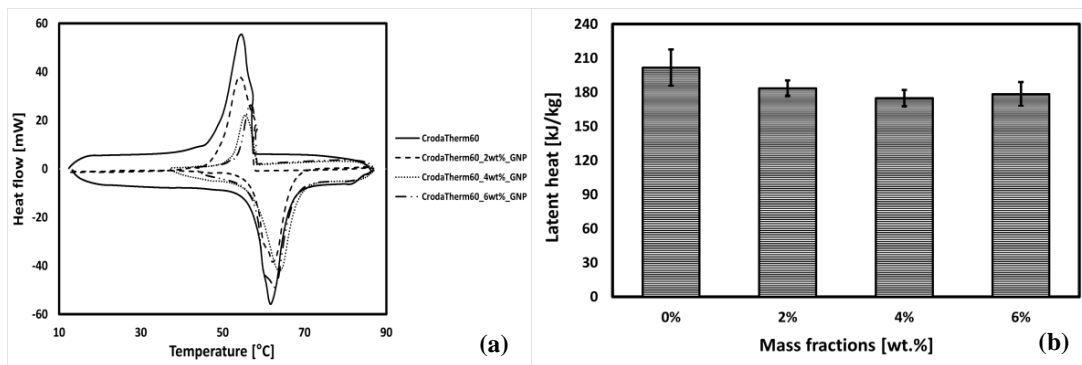

Fig. 4. (a) DSC curves of CrodaTherm60 and NePCMs and (b) difference in Latent heat capacity

The changes in the latent heat capacity with the increase in loadings of GNPs into the base PCM can be observed in Fig. 4 (b). As seen on Tab. 2 the latent heat increased with 6 wt.% when comparing with the NePCM with 4 wt.%, this could be explained due to the uncertainty of the measurements related to the precision of the balance used to weight the reference samples as well as the DSC equipment accuracy. Issues were also found when performing the DSC measurements, as there was leakage on the crucible pans from the samples, resulting in mass changes during the experiments.

3.3 Effects of the mass fraction on the densities

The density of CrodaTherm60 and NePCMs, with loadings of GNPs, at a solid state were experimentally measured and are show in Tab.3.

Tab. 3: Variation on the Density of the NePCMs with the incorporation of 2 nm GNPs

Material	Wt.%	Density (solid) [kg/m^3]	Standard deviation [kg/m^3]	Increase in density [%]
CrodaTherm60	0	937	±8.5	-
CrodaTherm60 + GNPs	2	949	±4.1	1.2
	4	974	±7.6	4.0
	6	996	±2.9	6.3

The effects of the GNPs mass fractions on the PCM density are illustrated in Fig. 5. The measured solid density of the CrodaTherm60 is 937 kg/m^3 which is 1.6% higher than the density reported by the suppliers, 922 kg/m^3. There is a strong linear correlation with a factor of 0.98, which indicates that the increase in the density of the NePCMs is directly proportional to the mass fraction of GNPs.
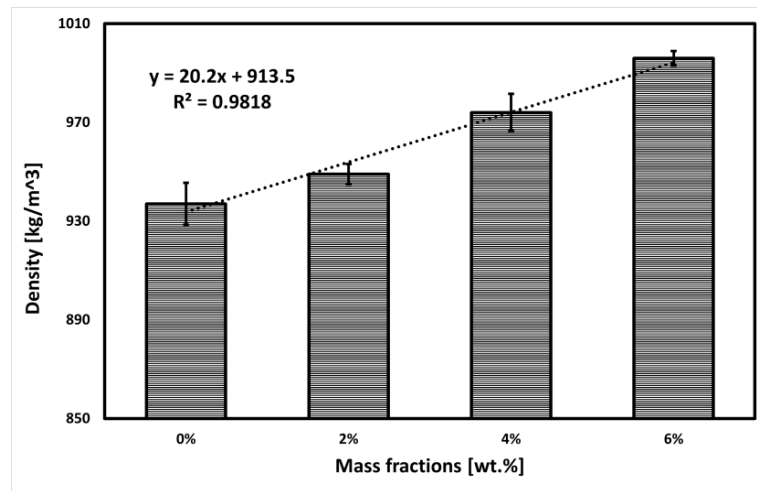

Fig. 5: Effects on the density with the increase of mass fractions wt.% of GNPs

3.4 Thermal conductivity

One of the performance indicators of the storage media material is the rate at which the energy can be stored and released, and it is highly dependent on the thermal conductivity of the material. Tab. 4 summarises the variation of the solid thermal conductivity of the CrodaTherm60 and NePCMs with different mass fractions, 2-4 wt.%, and the enhancement rates. The solid thermal conductivity measurements were taken at approximately 25 °C and for each sample, the tests were repeated 3 times and the value of each data is represented as mean ± standard deviation.

Tab. 4: Measured thermal conductivity in solid state at ambient temperature of CrodaTherm 60 with the incorporation of 2 nm GNPs

Material	Wt.%	Thermal conductivity [W/m.K]	Thermal conductivity enhancement [%]	Standard deviation [W/m.K]
CrodaTherm60	0	0.206	-	±0.021
CrodaTherm60 + GNPs	2	0.224	8.8	±0.007
	4	0.228	10.6	±0.011
	6	0.230	11.5	0.007

It can be seen from Fig. 6, that the thermal conductivity of the NePCMs increases along with the increase of GNPs contents. The thermal conductivity of the CrodaTherm60 was measured to be 0.206 W/m.K and the standard deviation in the measurement of thermal conductivity was up to 0.021 W/m.K. Although there was an increase in the thermal conductivity of the NePCMs, the thermal conductivity enhancement was lower than expected, despite the excellent thermal conductivity of the GNPs.
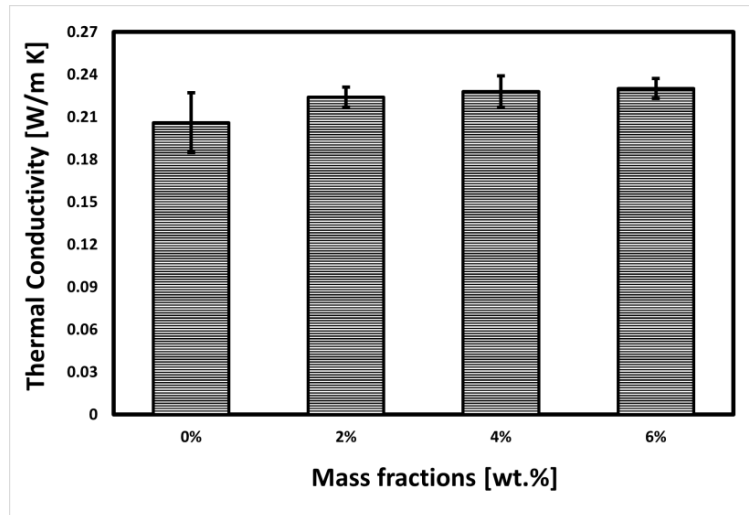
Fig. 6: Measured thermal conductivity of the solid NePCMs as a function of the loading of graphene nanoplatelets

Tab. 5 shows the results in the thermal conductivity enhancement in recent studies that have used carbon-based nanoparticles, mostly GNPs with similar geometries to the nanoparticles used in this study. There are significant discrepancies in the results reported in this study compared with previously published studies. The discrepancies could be attributed to numerous factors, some related to the differences in the nanocomposites, such as the size, thickness, specific surface area, and agglomeration of the nanoparticles and others related to the nonreported uncertainties in the measurements. The result reported in this study are preliminary; however, it is evident that the impact of carbon nanoparticles in the thermal conductivity should be further investigated.

Tab. 5: A summary of recent studies that used carbon-based nanomaterials as a conductive filler

Base PCM		Nanoparticles		NePCMs			Ref.
PCM/ T_m [°C]	k [W/m.K]	Type	Size	[wt.%]	k [W/m.K]	$K_{enhancement}$ [%]	
Paraffin [29-36°C]	0.20	GNPs	-	1	0.23	16 %	(Abdelrazik et al., 2020)
				5	0.24	20 %	
				10	0.26	28 %	
				20	0.30	47 %	
Palmitic-Stearic acid [54°C]	0.26	GNPs	Thickness: 4-20 nm Layers: <20 Size: 5-10µm	1	0.34	30 %	(Yuan et al., 2016b)
				2	0.44	65 %	
				4	0.62	134 %	
				8	0.98	273 %	
Myristic acid [54.4°C]	0.22	GNPs	Diameter: 5-10 µm Thickness: 3-10nm	1	0.45	104 %	(He et al., 2019)
				2	0.50	127 %	
				3	0.60	176 %	
n-nonacosane [61.6°C]	0.2	xGnP	-	2	0.75	25 %	(Shi et al., 2013)
				5	1.75	100 %	
				10	2.75	150 %	

A graphical comparison of the variation of the thermal conductivity of different carbon-based NePCMs as well as the current NePCMs prepared in this study is shown in Fig. 7. Yuan et al. (2016) investigated the thermal performance of palmitic-stearic acid with GNPs. The NePCMs were prepared using a similar synthesis process as the preparation process used in this study; however, the time taken for the magnetic stirring as well as the ultrasonication, were of 1 h each which was 30 min higher than the time taken for the preparation of the NePCMs in this study. This could have resulted in a better dispersion of the GNPs into the palmitic-stearic acid, resulting in less agglomeration. He et al. (2019) prepared and characterized myristic acid with different carbon nanoparticles including GNPs. The level of enhancement in the thermal conductivity with the increase of GNPs slowed down with the increase in the concentration of the nanoparticles.

The lower increase in the thermal conductivity of the NePCMs prepared in this study could be due to the agglomeration and sedimentation phenomena, and according to Xuan et al. (2003) the aggregation of the nanoparticles can have a negative impact on the thermal conductivity enhancement since Brownian motion will be slower. Although, the specific surface area of the nanomaterial play an important role in the shape stabilization of the PCMs, it can also accelerate the nanomaterial aggregation, which tends to weaken the thermal conductivity enhancement effect. The specific surface area of the GNPs used in this study is 750 m^2/g, thus, the low increase in the thermal conductivity could have been attributed to this phenomenon. Therefore, methods should be taken to avoid the aggregating issues that can be caused by the agglomeration and sedimentation issues.
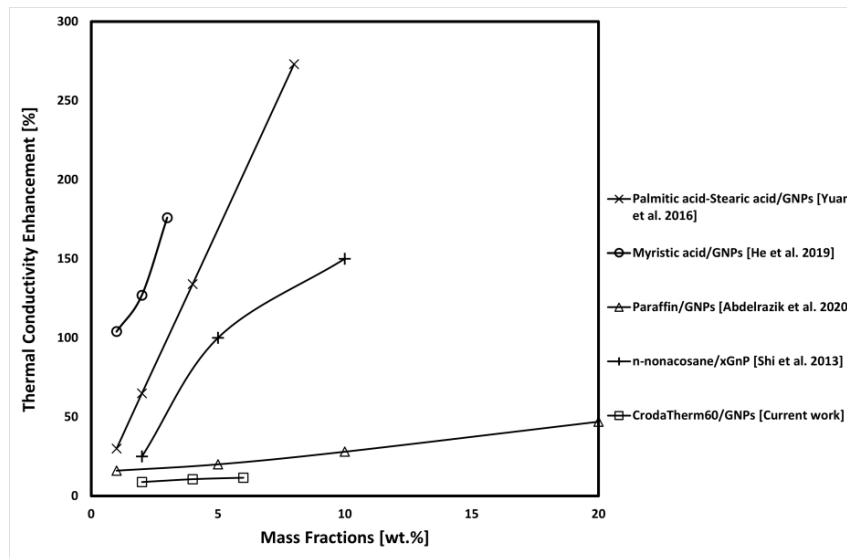

Fig. 7: Comparison of thermal conductivity enhancements of NePCMs vs additive mass fractions (wt.%) using carbon based nanomaterials

4. Conclusion

In this paper, the effects of adding graphene nanoplatelets in the main properties, phase change temperatures, latent heat capacities, density, and thermal conductivities of the CrodaTherm60 were investigated. The latent heat capacity of the NePCMs significantly decreased with the addition of GNPs into the CrodaTherm60 and the content of nanoparticles. The measured melting temperature of 57.2 °C and high latent heat capacity of 201.7 kJ/kg make this material suitable for space and domestic water heating applications. Due to weigh loss reported from the samples analysed through the DSC characterization, more samples using different crucibles are going to be prepared and analysed to reduce the error and uncertainties from the measurements taken. The GNPs were very ineffective in boosting the thermal conductivity of the CrodaTherm60 despite its high thermal conductivity. This can be associated to the high specific surface area of the GNPs which can be prone for agglomeration and sedimentation issues, seen from the SEM images taken from the NePCMs samples. Therefore, further efforts will be required to address the agglomeration issues, which might include increasing the time for ultrasonication during the preparation process to break the GNPs clusters as well as using nucleating agents to improve the dispersion of the nanoparticles into the PCM.

5. Credit author statement

Elisangela Jesus D'Oliveira: Conceptualization, Methodology, Data acquisition, Writing – original draft.
Sol Carolina Costa Pereira: Supervision, Data acquisition, Methodology, Writing -review & editing.
Ulugbek Azimov: Review & Editing. **Dominic Groulx:** Review & Editing.

6. Acknowledgements

7. References

Abdelrazik, A., Al-Sulaiman, F. & Saidur, R. 2020. Numerical investigation of the effects of the nano-enhanced phase change materials on the thermal and electrical performance of hybrid PV/thermal systems. *Energy Conversion and Management,* 205**,** 112449.

Amin, M., Putra, N., Kosasih, E. A., Prawiro, E., Luanto, R. A. & Mahlia, T. 2017. Thermal properties of beeswax/graphene phase change material as energy storage for building applications. *Applied Thermal Engineering,* 112**,** 273-280.

Cui, W., Yuan, Y., Sun, L., Cao, X. & Yang, X. 2016. Experimental studies on the supercooling and melting/freezing characteristics of nano-copper/sodium acetate trihydrate composite phase change materials. *Renewable Energy,* 99**,** 1029-1037.

D'oliveira, E. J., Pereira, S. C. C., Groulx, D. & Azimov, U. 2022. Thermophysical properties of Nano-enhanced phase change materials for domestic heating applications. *Journal of Energy Storage,* 46**,** 103794.

Fadl, M. & Eames, P. C. 2021. Thermal performance evaluation of a latent heat thermal energy storage unit with an embedded multi-tube finned copper heat exchanger. *Experimental Heat Transfer***,** 1-20.

Feng, L., Wu, J., Sun, W. & Cai, W. 2022. Effects of Pore Structure and Pore Size of Expanded Graphite on the Properties of Paraffin Wax/Expanded Graphite Composite Phase Change Materials. *Energies,* 15**,** 4201.

He, M., Yang, L., Lin, W., Chen, J., Mao, X. & Ma, Z. 2019. Preparation, thermal characterization and examination of phase change materials (PCMs) enhanced by carbon-based nanoparticles for solar thermal energy storage. *Journal of Energy Storage,* 25**,** 100874.

Hu, X., Huang, H., Hu, Y., Lu, X. & Qin, Y. 2021. Novel bio-based composite phase change materials with reduced graphene oxide-functionalized spent coffee grounds for efficient solar-to-thermal energy storage. *Solar Energy Materials and Solar Cells,* 219**,** 110790.

Jeong, S.-G., Chung, O., Yu, S., Kim, S. & Kim, S. 2013. Improvement of the thermal properties of Bio-based PCM using exfoliated graphite nanoplatelets. *Solar Energy Materials and Solar Cells,* 117**,** 87-92.

Liu, L., Fan, X., Zhang, Y., Zhang, S., Wang, W., Jin, X. & Tang, B. 2020. Novel bio-based phase change materials with high enthalpy for thermal energy storage. *Applied energy,* 268**,** 114979.

Manoj Kumar, P., Mylsamy, K. & Saravanakumar, P. 2020. Experimental investigations on thermal properties of nano-SiO2/paraffin phase change material (PCM) for solar thermal energy storage applications. *Energy Sources, Part A: Recovery, Utilization, and Environmental Effects,* 42**,** 2420-2433.

Müller, L., Rubio-Pérez, G., Bach, A., Muñoz-Rujas, N., Aguilar, F. & Worlitschek, J. 2020. Consistent DSC and TGA Methodology as Basis for the Measurement and Comparison of Thermo-Physical Properties of Phase Change Materials. *Materials,* 13**,** 4486.

Okogeri, O. & Stathopoulos, V. N. 2021. What about greener phase change materials? A review on biobased phase change materials for thermal energy storage applications. *International Journal of Thermofluids***,** 100081.

Prado, J. I. & Lugo, L. 2020. Enhancing the thermal performance of a stearate phase change material with graphene nanoplatelets and MgO nanoparticles. *ACS applied materials & interfaces,* 12**,** 39108-39117.

Putra, N., Amin, M., Kosasih, E. A., Luanto, R. A. & Abdullah, N. A. 2017. Characterization of the thermal stability of RT 22 HC/graphene using a thermal cycle method based on thermoelectric methods. *Applied Thermal Engineering,* 124**,** 62-70.

Sang, M., Shin, J., Kim, K. & Yu, K. J. 2019. Electronic and thermal properties of graphene and recent advances in graphene based electronics applications. *Nanomaterials,* 9**,** 374.

Shi, J.-N., Ger, M.-D., Liu, Y.-M., Fan, Y.-C., Wen, N.-T., Lin, C.-K. & Pu, N.-W. 2013. Improving the thermal conductivity and shape-stabilization of phase change materials using nanographite additives. *Carbon,* 51**,** 365-372.

Wang, C., Feng, L., Li, W., Zheng, J., Tian, W. & Li, X. 2012. Shape-stabilized phase change materials based on polyethylene glycol/porous carbon composite: the influence of the pore structure of the carbon materials. *Solar Energy Materials and Solar Cells,* 105**,** 21-26.

Wuliu, Y., Liu, J., Zhang, L., Wang, S., Liu, Y., Feng, J. & Liu, X. 2021. Design of bio-based organic phase change materials containing a "safety valve". *Green Chemistry,* 23**,** 8643-8656.

Xuan, Y., Li, Q. & Hu, W. 2003. Aggregation structure and thermal conductivity of nanofluids. *AIChE Journal,* 49**,** 1038-1043.

Yu, S., Jeong, S.-G., Chung, O. & Kim, S. 2014. Bio-based PCM/carbon nanomaterials composites with enhanced thermal conductivity. *Solar Energy Materials and Solar Cells,* 120**,** 549-554.

Yuan, Y., Li, T., Zhang, N., Cao, X. & Yang, X. 2016a. Investigation on thermal properties of capric–palmitic–stearic acid/activated carbon composite phase change materials for high-temperature cooling application. *Journal of Thermal Analysis and Calorimetry,* 124**,** 881-888.

Yuan, Y., Zhang, N., Li, T., Cao, X. & Long, W. 2016b. Thermal performance enhancement of palmitic-stearic acid by adding graphene nanoplatelets and expanded graphite for thermal energy storage: A comparative study. *Energy,* 97**,** 488-497.

Zhang, Z., Duan, Z., Chen, D., Xie, Y., Cao, X. & Wang, J. 2021. Sodium acetate trihydrate-based composite phase change material with enhanced thermal performance for energy storage. *Journal of Energy Storage,* 34**,** 102186.